MCB
Journals.ASM.org

Insertion of an Imprinted Insulator into the *IgH* Locus Reveals Developmentally Regulated, Transcription-Dependent Control of V(D)J Recombination

Nadine Puget,[a,b] Ryutaro Hirasawa,[c*] Ngoc-Sa Nguyen Hu,[a,b] Nathalie Laviolette-Malirat,[a,b] Robert Feil,[c] Ahmed Amine Khamlichi[a,b]

CNRS UMR5089, Institut de Pharmacologie et de Biologie Structurale (IPBS), Toulouse, France[a]; Université de Toulouse, UPS, Institut de Pharmacologie et de Biologie Structurale (IPBS), Toulouse, France[b]; Institute of Molecular Genetics (IGMM), CNRS UMR5535, and University of Montpellier I & II, Montpellier, France[c]

The assembly of antigen receptor loci requires a developmentally regulated and lineage-specific recombination between variable (V), diversity (D), and joining (J) segments through V(D)J recombination. The process is regulated by accessibility control elements, including promoters, insulators, and enhancers. The *IgH* locus undergoes two recombination steps, D-J_H and then V_H-DJ_H, but it is unclear how the availability of the DJ_H substrate could influence the subsequent V_H-DJ_H recombination step. The Eμ enhancer plays a critical role in V(D)J recombination and controls a set of sense and antisense transcripts. We epigenetically perturbed the early events at the *IgH* locus by inserting the imprinting control region (ICR) of the *Igf2/H19* locus or a transcriptional insulator devoid of the imprinting function upstream of the Eμ enhancer. The insertions recapitulated the main epigenetic features of their endogenous counterparts, including differential DNA methylation and binding of CTCF/cohesins. Whereas the D-J_H recombination step was unaffected, both the insulator insertions led to a severe impairment of V_H-DJ_H recombination. Strikingly, the inhibition of V_H-DJ_H recombination correlated consistently with a strong reduction of DJ_H transcription and incomplete demethylation. Thus, developmentally regulated transcription following D-J_H recombination emerges as an important mechanism through which the Eμ enhancer controls V_H-DJ_H recombination.

Monoallelic gene expression in mammals is a hallmark of various complex processes, including X-chromosome inactivation in female cells, genomic imprinting, and allelic exclusion at antigen receptor loci (1, 2). In genomic imprinting, the allelic expression of a subset of genes depends on the parental origin of the allele and is controlled by specialized *cis*-regulatory elements called imprinting control regions (ICRs) (3). One of the best-studied imprinted domains is the *Igf2/H19* locus, which is regulated by an ICR methylated on its paternally inherited copy. The unmethylated maternal copy is bound by the zinc finger protein CTCF and cohesins, leading to the insulation of the flanking *Igf2* gene from enhancer sequences located downstream of the *H19* gene (3).

Although X-chromosome inactivation, genomic imprinting, and allelic exclusion use common epigenetic mechanisms (1), they clearly display different features as well. Particularly, allelic exclusion additionally involves a unique developmentally regulated recombination process in B and T lymphocytes, called V(D)J recombination. This process is catalyzed by the lymphoid-specific recombinase complex RAG1/RAG2, which recognizes conserved recombination signal sequences (RSSs) flanking the variable (V), diversity (D), and joining (J) segments in the variable domain of antigen receptor (*IgH*, *IgL*, and *TCR*) loci (4–6).

The ~3-Mb mouse *IgH* locus contains 195 V_H genes spanning ~2.5 Mb (7). The V_H genes are subdivided into V_H gene families, including the distal V_H genes (V_{HJ558} and V_{H3609}) and the proximal V_H genes (V_{HQ52} and V_{H7183}). The V_H genes are followed by a dozen D segments (~60 kb), 4 J_H segments (~2 kb), and 8 constant genes (~200 kb) (7, 8).

The generation of the primary immunoglobulin repertoire involves developmentally ordered recombination steps. D-J_H recombination occurs on both *IgH* alleles, before the initiation of V_H-DJ_H joining on one of the two *IgH* alleles only. If productive, this produces a μ heavy chain that signals the arrest of the rearrangement on the opposite *IgH* allele (4, 6).

The ordered rearrangement of the IgH gene segments is associated with various transcriptional events and chromatin modifications and is controlled to a large extent by accessibility control elements, including enhancers, insulators, and promoters, in a cell type- and developmental stage-specific manner (4, 9). Two regulatory elements in the *IgH* locus were shown to control V(D)J recombination. The Eμ enhancer, located between the variable and the constant domains, plays a critical role in V(D)J recombination and associated germ line transcription. Deletion of Eμ affects D-J_H recombination partially and V_H-DJ_H recombination much more severely (10, 11). Eμ also controls the expression of a set of sense transcripts (STs) and antisense transcripts (ASTs) at specific sites of the *IgH* variable locus (10–14). The STs include Iμ transcripts derived from the Eμ enhancer and μ0 transcripts ini-

Received 17 February 2014 **Returned for modification** 12 March 2014
Accepted 10 November 2014

Accepted manuscript posted online 17 November 2014

Citation Puget N, Hirasawa R, Hu N-SN, Laviolette-Malirat N, Feil R, Khamlichi AA. 2015. Insertion of an imprinted insulator into the *IgH* locus reveals developmentally regulated, transcription-dependent control of V(D)J recombination. Mol Cell Biol 35:529–543. doi:10.1128/MCB.00235-14.

Address correspondence to Robert Feil, robert.feil@igmm.cnrs.fr, or Ahmed Amine Khamlichi, ahmed.khamlichi@ipbs.fr.

* Present address: Ryutaro Hirasawa, RIKEN BioResource Center, Koyadai, Tsukuba, Ibaraki, Japan.

Supplemental material for this article may be found at http://dx.doi.org/10.1128/MCB.00235-14.

doi:10.1128/MCB.00235-14

tiated from the D_{Q52} promoter upstream of the 3′-most D segment. ASTs are initiated within the J_H-Eμ region (12, 14) and from an ill-defined antisense promoter within the D cluster (15). Deletion of Eμ also affects germ line transcription of the 3′-most V_H segments of the proximal V_H domain (13).

Additionally, CTCF-binding elements (CBEs) with insulator activity were identified between the V_H and the D clusters (16, 17). Deletion of these CTCF sites within this intergenic control region (IGCR1) led to increased germ line transcription and recombination of the proximal V_H genes and perturbed the order and the cell type specificity of V(D)J recombination, as well as feedback regulation of the proximal V_H segments (18).

The *IgH* locus undergoes two recombination steps, D-J_H and then V_H-DJ_H recombination, and it remains unknown how the status of the DJ_H substrate influences the subsequent V_H-DJ_H recombination step and what the role of the Eμ enhancer in this process could be. To address this key question, we inserted upstream of the Eμ enhancer either the ICR of the imprinted *Igf2/H19* locus or the transcriptional insulator of the chicken β-globin locus (cHS4), devoid of imprinting function, and analyzed their effects on V(D)J recombination and associated germ line transcription. We found that both the insulators strongly affect V_H-to-DJ_H recombination in developing B cells. This marked phenotype was linked to pronounced transcriptional changes and aberrant DNA methylation at the DJ_H segment following D-J_H recombination. This main finding strongly suggests that local transcriptional and epigenetic changes following the first step of recombination modulate the occurrence of the subsequent V_H-to-DJ_H recombination step.

MATERIALS AND METHODS

Mice. The experiments on mice were carried out according to CNRS ethical guidelines and approved by the Midi-Pyrénées Regional Ethical Committee.

Gene targeting. For the targeting constructs, a ~2.4-kb BglII fragment containing the 4 CTCF sites of the ICR or a ~2.6-kb XbaI fragment containing 2 cHS4 CTCF sites was first cloned into the BamHI site or the XbaI site of a modified pBluescript II KS(−) vector (Stratagene) containing an ~1.3-kb floxed neomycin resistance [*Neo*^{r}] cassette. The inserts (ICR plus the *Neo*^{r} cassette or cHS4 plus the *Neo*^{r} cassette) were taken out as a blunt end or a ClaI fragment, respectively, and inserted into a blunt end or a ClaI site that replaced the unique NaeI site between Eμ and J_{H4} in the PA14 vector (kindly provided by M. Cogné, CNRS, Limoges, France) containing the sequence between the EcoRI site (upstream of D_{Q52}) and AseI (in the 5′ part of Sμ). The AseI site was modified into the NotI site and subsequently used to insert the herpes simplex virus *tk* gene. The ES cell line CK35 (strain 129Sv; kindly provided by C. Kress, Institut Pasteur, Paris, France) was transfected by electroporation and selected using G418 (300 μg/ml) and ganciclovir (2 μM). Recombinant clones were identified by PCR and Southern blot analysis after BamHI (ICR construct) or KpnI (cHS4 construct) digestion with an external 3′ probe spanning the Cμ1 exon. Two ES clones showing homologous recombination were injected into C57BL/6 mouse blastocysts. The male chimera mice were then mated with C57BL/6 female mice in order to derive permanent mouse lines. Germ line transmission of the mutation was checked by PCR and Southern blotting after BamHI or KpnI digestion and by use of the same external probe. Homozygous N/N mutant mice were mated with EIIa-cre transgenic mice. The progeny were checked by PCR for *Cre*-mediated deletion of the *Neo*^{r} cassette. Additional checks were made by sequencing pertinent regions in the genomic DNA (see Fig. S1 in the supplemental material).

Antibodies. Phycoerythrin (PE)-conjugated anti-IgM^b, fluorescein isothiocyanate (FITC)-conjugated anti-IgM^a, PE-conjugated anti-CD43, FITC-conjugated anti-κ, and FITC- and PE-conjugated anti-AA4.1 were purchased from BD Pharmingen. Allophycocyanin-conjugated anti-B220 and FITC- and PE-conjugated anti-IgM were from BioLegend. Anti-CTCF was purchased from Millipore, and anti-SMC1 was from Bethyl.

Fluorescence-activated cell sorting (FACS) analyses. Single-cell suspensions from bone marrows and spleens from 6- to 8-week-old mice were prepared by standard techniques. Cells (5×10^5 cells/assay) were stained and gated as indicated in the appropriate figure legends. Data on 2.0×10^4 viable cells were obtained by using a BD FACSCalibur flow cytometer. Dead cells were excluded by labeling with propidium iodide.

DNA methylation analyses. Splenic B cells were negatively sorted by using CD43 magnetic microbeads and LS columns (Miltenyi). Total bone marrow B cells were sorted by using CD19 magnetic microbeads and LS columns (Miltenyi). Genomic DNAs were extracted and subjected to methylation-sensitive restriction enzyme digestion (MSRED) followed by quantitative PCR (qPCR) or assayed by sodium bisulfite sequencing by using a bisulfite conversion kit (Active Motif). The primers used are listed in Table S1 in the supplemental material.

ChIP. Chromatin was prepared from sorted splenic B cells, and chromatin immunoprecipitation (ChIP) was carried out as described previously (19).

V(D)J rearrangement assays. Pro-B cells were sorted from bone marrow by using CD19 magnetic microbeads and LS columns (Miltenyi), labeled with anti-B220, anti-CD43, and anti-κ, and sorted as the B220-positive (B220$^+$), κ-negative (κ$^-$), and CD43^{high} fraction. The purity of the sorted population was checked by FACS and by the rearrangement status of the κ locus. Splenic B cells were sorted by using CD43 magnetic microbeads and LS columns (Miltenyi). The CD4$^+$ CD8$^+$ thymocytes were sorted as described previously (18). Genomic DNAs from the sorted cell populations were prepared by standard techniques and diluted for the semiquantitative PCR or the qPCR assays. For quantification, agarose gels were dried for 1 h at 80°C using a gel dryer (Bio-Rad), stained with SYBR green I (Invitrogen) for 1 h, and scanned by using a PhosphorImager (Molecular Dynamics). After subtracting the background levels, the signals corresponding to the recombination products (DJ_H or V_HDJ_H) in the diluted lanes were normalized against the HS4 signals. The histograms show the average for the four recombination products.

Reverse transcription-qPCR (RT-qPCR). Pro-B cells from Rag2$^{-/-}$ mouse (strain 129Sv) bone marrow were sorted using CD19 magnetic microbeads (Miltenyi). Single IgM^a- or IgM^b-expressing B cells were sorted after staining with anti-B220$^+$, anti-AA4.1-positive (anti-AA4.1$^+$), and anti-IgM^a (or anti-IgM^b) antibodies. Total RNAs were reverse transcribed (Invitrogen) and subjected to semiquantitative PCR, using SYBR green I (Invitrogen) and ImageQuant software, or to qPCR, using Sso Fast Eva Green (Bio-Rad).

Statistical analysis. Results are expressed as the mean ± standard error of the mean (GraphPad Prism), and overall differences between wild-type (WT) and mutant mice were evaluated by the analysis of variance parametric test with the Newman-Keuls posttest or the Kruskal-Wallis nonparametric test with Dunn's posttest. The difference between means was significant if the P value was <0.05, very significant if the P value was <0.01, and extremely significant if the P value was <0.001.

RESULTS

In the analyses described below, the homozygous mice are denoted *ICR/ICR* and *cHS4/cHS4*. In hemizygous mice, *ICR/+* and *+/ICR* indicate the maternal and paternal origins of the mutant allele, respectively. Since no parent-of-origin effects on B cell development were found in cHS4 hemizygous mice (see Fig. 3; also see Fig. S3 in the supplemental material), analyses of these mice were performed regardless of the parental origin of the cHS4 insert.

Acquisition of paternal allele-specific DNA methylation at the ectopic ICR. Since the *H19* ICR acquires paternal allele-specific DNA methylation during spermatogenesis (20), we deter-

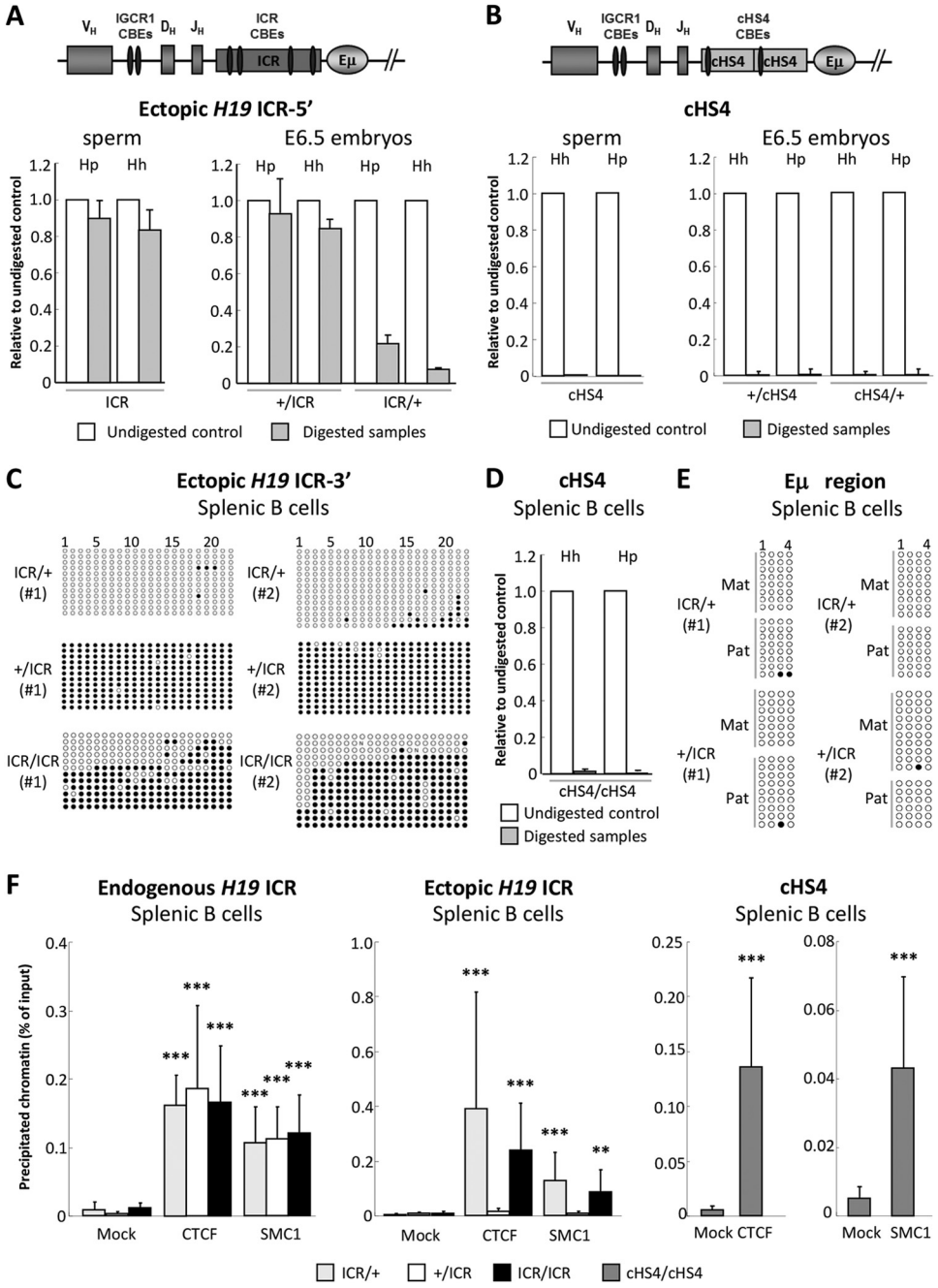

FIG 1 DNA methylation and CTCF/cohesin binding at the ectopic ICR and cHS4. (A, B) The schemes at the top show the CBEs within the ectopic inserts and the upstream endogenous IGCR1 CBEs. Not all CBEs within the *IgH* locus are shown. Genomic DNAs from sperm (left) and E6.5 embryos (right) of ICR (A) and cHS4 mice (B) were analyzed by MSRED/qPCR at the 5′ part of the inserts. Hh, HhaI digestion; Hp, HpyCH4IV digestion. Note that after enzymatic digestion, the intact methylated DNA was quantified by qPCR by comparison to the undigested samples ($n = 3$). (C) Genomic DNAs from sorted ICR splenic B cells with the indicated genotypes were analyzed by bisulfite sequencing. Methylated (filled circles) and unmethylated (open circles) cytosines within 22 CpGs at the 3′ part of the ectopic *H19* ICR from two independent experiments are displayed. (D) Genomic DNA from sorted *cHS4/cHS4* splenic B cells was analyzed as described in the legend to panel B ($n = 3$). (E) Bisulfite sequencing of 4 CpGs downstream of Eμ in genomic DNAs from sorted hemizygous ICR splenic B cells. Mat, maternal; Pat, paternal. (F) CTCF and cohesin binding to the ectopic ICR and cHS4 in B cells. Chromatin from purified splenic B cells with the indicated genotypes was immunoprecipitated with anti-CTCF or anti-SMC1 antibodies. ChIP-qPCR was performed on the endogenous *H19* ICR (left), the ectopic ICR (middle), and the ectopic cHS4 (right). The histograms show the standard deviations ($n = 4$ for ICRs, $n = 3$ for cHS4). ***, $P < 0.001$; **, $P < 0.01$.

mined whether the ectopically inserted *H19* ICR also acquired parent-of-origin-specific DNA methylation. Genomic DNA from sperm and day 6.5 (E6.5) embryos was analyzed by methylation-sensitive restriction enzyme digestion followed by qPCR (MSRED/qPCR). We assayed two CpG dinucleotides at the upstream part of the ICR insert and found that these are fully methylated in sperm (Fig. 1A). This paternal methylation was stably maintained in E6.5 embryos (Fig. 1A). Upon maternal inheri-

tance, hardly any DNA methylation was detected at the ectopic ICR in E6.5 embryos (Fig. 1A).

The cHS4 insulator binds CTCF (21) but has no imprinting function and was reported to remain hypomethylated at ectopic sites (22, 23). Concordantly, at four analyzed CpGs at the 5′ part of the ectopic cHS4, there was an absence of DNA methylation in sperm and E6.5 embryos, regardless of the parental origin of the cHS4 insert (Fig. 1B).

DNA methylation and CTCF/cohesin binding at the ectopic ICR in B cells. Our finding of imprinted DNA methylation at the ectopic ICR in embryos did not preclude the possibility that these marks could be lost during B cell development, for instance, through a demethylating activity of the Eμ enhancer (24, 25).

Therefore, we analyzed by bisulfite sequencing and MSRED/qPCR the DNA methylation pattern of the ectopic ICR and cHS4 in purified splenic cells. In hemizygous B cells, the ectopic ICR DNA was highly methylated only when inherited from the father (*+/ICR*) (Fig. 1C). In homozygous *ICR/ICR* B cells, concordantly, about 50% methylation was detected (Fig. 1C). The ectopic cHS4, in contrast, was fully unmethylated in homozygous B cells (Fig. 1D).

To ascertain that DNA methylation at the ectopic ICR had not spread into the Eμ region, we assessed by bisulfite sequencing four CpGs located at the 3′ side of Eμ. This did not reveal any DNA methylation in hemizygous B cells, showing that this region had remained unmethylated (Fig. 1E).

To investigate whether the ectopic ICR and cHS4 were bound by CTCF and SMC1 (a subunit of the cohesin complex), we performed chromatin immunoprecipitation (ChIP)-qPCR. Chromatin was prepared from either hemizygous or homozygous splenic B cells. As an internal control, we studied the endogenous ICR. We focused on the ICR's fourth CTCF-binding site and used different backward primers which distinguish the ectopic and the endogenous ICR. CTCF and SMC1 were readily immunoprecipitated from the endogenous ICR (Fig. 1F, left). Also, the maternally inherited copy of the ectopic ICR bound CTCF and SMC1, whereas the paternal copy did not (Fig. 1F, middle). Concordantly, CTCF and SMC1 were immunoprecipitated in homozygous *ICR/ICR* B cells as well (Fig. 1F, middle).

ChIP-qPCR of homozygous B cells revealed binding of CTCF and SMC1 to the ectopic cHS4 as well (Fig. 1F, right). Although we did not perform the assay allele specifically, the ChIP data, together with those on DNA methylation (Fig. 1D) and B cell development in hemizygotes (see below), led us to infer that the ectopic cHS4 bound CTCF and SMC1 regardless of its parental origin.

Together, these data show parental allele-specific DNA methylation and CTCF/SMC1 binding at the ectopic ICR, which was stably maintained in B cells. Also, the ectopic cHS4 bound CTCF/SMC1 and remained fully unmethylated in B cells.

V_H-DJ_H recombination, but not D-J_H recombination, is altered in homozygous mutant mice. Analysis of the bone marrow of homozygous mice revealed an accumulation of pro-B cells (see Fig. S3 in the supplemental material), suggesting that V(D)J recombination, normally completed at this developmental stage, was impaired. We therefore investigated if and at which step V(D)J recombination was compromised.

We quantified the proportion of the D_{Q52} and J_{H1} segments that had retained their unrearranged configuration (Fig. 2A, top). We found no difference in the total proportions of unrearranged D_{Q52} and J_{H1} segments between ICR, cHS4, and WT controls (Fig. 2A), suggesting that a similar number of alleles underwent D-J_H recombination.

Next, we performed a standard V(D)J recombination assay, which detects the recombined DJ_H segments. We used a forward primer that recognizes most D segments and a backward primer downstream of the J_{H4} segment (Fig. 2B, top). We found a slight accumulation of DJ_H segments in mutant pro-B cells (Fig. 2B, left and right), indicating that the D-J_H recombination step was not impaired by the insertions.

We then asked whether the mutations affected V_H-DJ_H recombination. For this, genomic DNA from sorted pro-B cells was subjected to semiquantitative PCR amplification of recombined V_H-DJ_H segments. A reduction of V_H-DJ_H recombination was detected in *ICR/ICR* and *cHS4/cHS4* pro-B cells at both proximal and distal V_H genes. This reduction was most pronounced in *ICR/ICR* pro-B cells (Fig. 2B, left and right).

Thus, homozygous insertion of the ICR or the cHS4 upstream of Eμ was not by itself incompatible with V(D)J recombination. The slight accumulation of D-J_H recombination events correlated with a reduction of V_H-DJ_H recombination, with no evidence for a differential effect on proximal versus distal V_H gene recombination. Moreover, insertion of the ICR or cHS4 upstream of Eμ did not perturb the order of rearrangements or the strict B cell type specificity of *IgH* V_H-DJ_H recombination (see Fig. S4 in the supplemental material).

Allelic exclusion and competition in hemizygous ICR and cHS4 mice. While the analyses on homozygous mice indicated an inefficiency of the mutant alleles to drive normal B cell development (see Fig. S3 in the supplemental material), the findings could have been blurred by cellular selection (26). In addition, this analysis was not informative with regard to the actual contribution of the mutant allele to B cell development, when put in competition with the WT allele.

In hemizygous animals, no significant difference from the WT controls was observed regardless of the parental origin of the ectopic ICR or cHS4 (Fig. 3A and B). Still, this normal development could have masked an altered allelic exclusion or an impaired expression of the mutant allele, which could have been compensated for by the WT allele.

To analyze more closely allelic exclusion and competition between WT and mutant alleles, we bred the mutant mice, which express an IgM^a allotype (they are derived from strain 129Sv), with WT C57BL/6 mice (which express an IgM^b allotype). As an additional control, we used B1-8 mice, in which the D_{Q52}-J_H region is replaced by a prerearranged V(D)J exon expressing IgM^a, leading to a complete exclusion of the WT allele (27). FACS analyses were performed by using monoclonal antibodies (MAbs) which readily distinguished between the IgM products of the two parental alleles.

Strikingly, the mutant allele from either *ICR/+* or *+/ICR* mice was totally excluded, and this exclusion pattern was stably maintained in the spleen (Fig. 3C). In *cHS4/+* mice, IgM^b-expressing B cells clearly outnumbered IgM^a-expressing B cells, with no evidence for allelic inclusion, as no cells double expressing IgM^a and IgM^b at levels above the background levels were detected. Also here, a similar pattern was found in the spleen (Fig. 3C).

Thus, when put in competition with the WT allele, the mutant *ICR* allele was impotent in driving B cell development and was totally excluded, regardless of its parental origin. The defect was

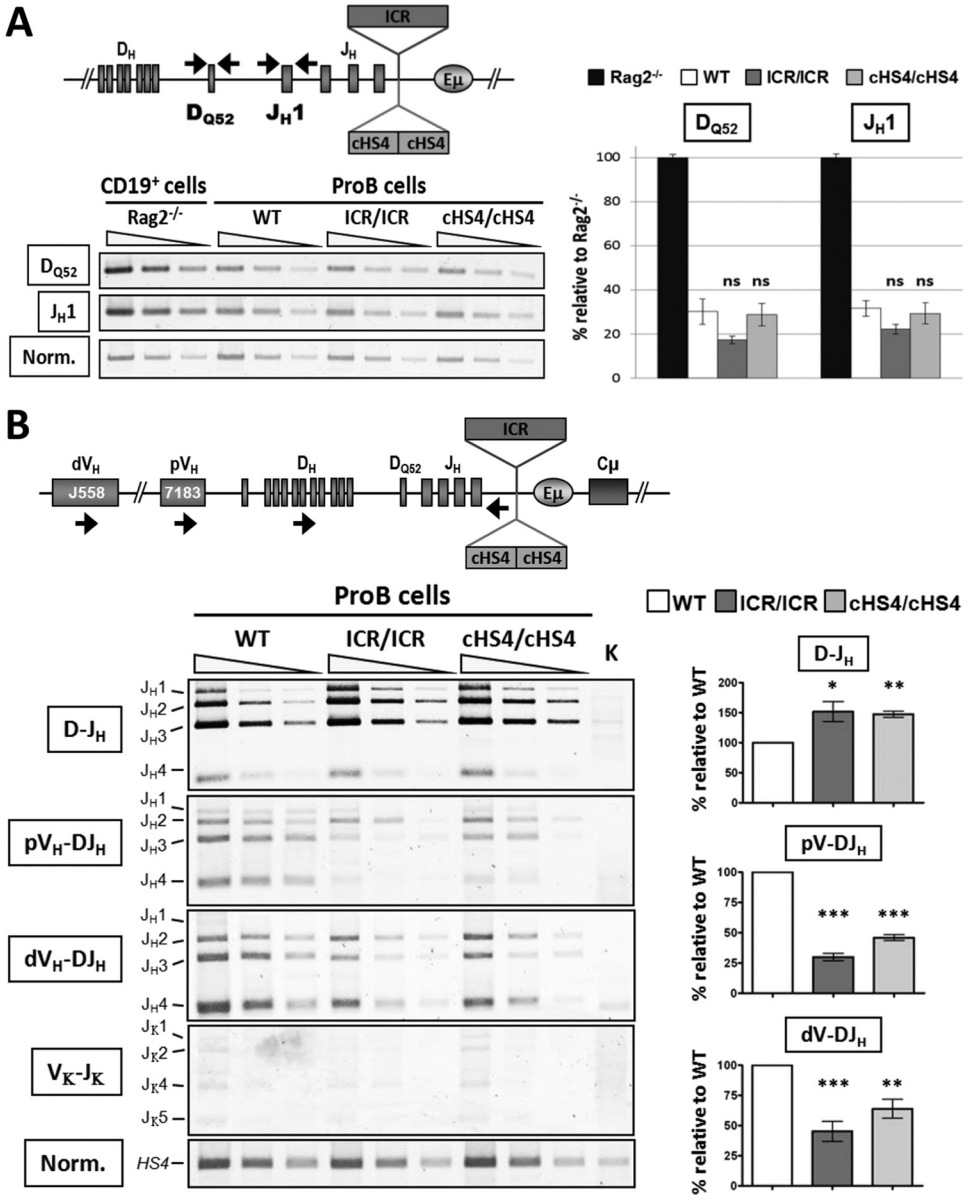

FIG 2 V(D)J recombination is altered in homozygous mutant mice. (A) Genomic DNAs were prepared from sorted pro-B cells with the indicated genotypes and subjected to PCR to amplify unrearranged D_{Q52} and J_{H1} gene segments. The relative position of the primers is indicated in the scheme at the top. PCR products were detected and quantified using genomic DNA from *Rag2*$^{-/-}$ mice, which do not undergo V(D)J recombination, as a control (100% of the signal). PCR of the HS4 enhancer of the 3′ regulatory region was performed for normalization of the DNA input. (Left) Semiquantitative PCR was performed on serial 3-fold dilutions; (right) amplification of unrearranged D_{Q52} and J_{H1} gene segments by qPCR. The histograms show the standard errors ($n = 4$). ns, not significant. (B) Genomic DNAs were prepared from sorted pro-B cells and subjected to semiquantitative PCR to amplify D-J_H, V_H-DJ_H, and Vκ-Jκ rearrangements using primers that bind the indicated gene segments and primers that pair 3′ of J_{H4} for the *IgH* locus (scheme at the top) or 3′ of Jκ5 for the κ locus. dV_H, distal VH; pV_H, proximal V_H. (Left) PCR was performed on serial 3-fold dilutions. Kidney (K) DNA was used as a negative control, and normalization (Norm.) was as described in the legend to panel A. (Right) Quantification of D-J_H and V_H-DJ_H rearrangements. The histograms show the standard errors ($n = 6$). ***, $P < 0.001$; **, $P < 0.01$; *, $P < 0.05$.

clearly less severe in the case of the mutant *cHS4* allele, with no evidence for a breakdown of allelic exclusion.

The hemizygous ICR and cHS4 insertions specifically affect V_H-DJ_H recombination. Next, we analyzed V(D)J recombination in an allele-specific manner in the hemizygous ICR mice, where selection pressure on the mutant allele is less stringent than that in the homozygous mice, as B cell development can be driven by the WT allele.

Genomic DNA was prepared from sorted pro-B cells and subjected to PCR using the same forward primers for all the genotypes. Backward primers were designed so that they preferentially amplified the WT allele or specifically amplified the mutant allele (Fig. 4A). Interestingly, D-J_H recombination was readily detected on the mutant *ICR* allele, regardless of its parental origin, and on the mutant *cHS4* allele (Fig. 4B and C). In contrast, only low levels of V_H-DJ_H recombination were detectable for both prox-

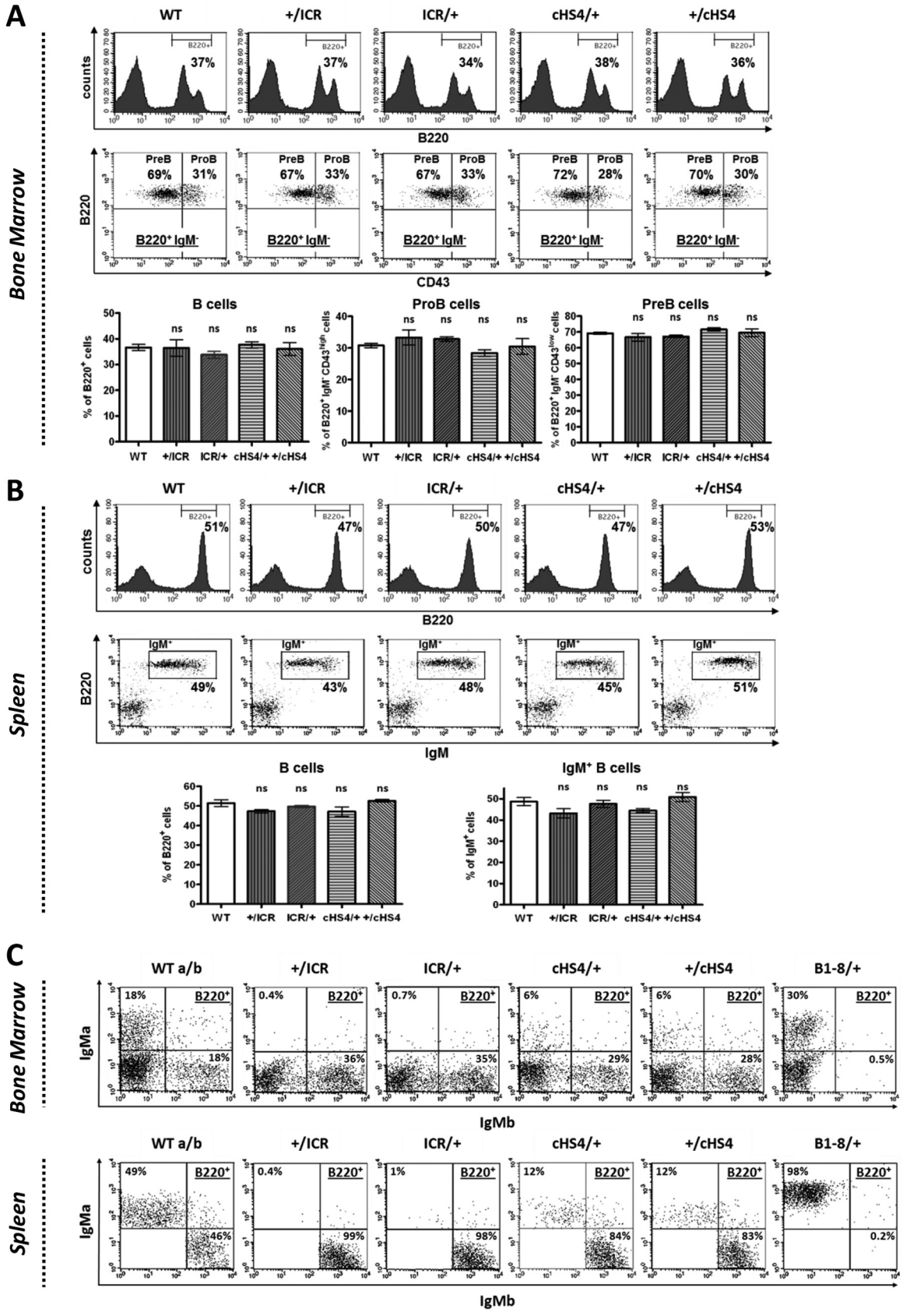
A
Bone Marrow
WT
+/ICR
ICR/+
cHS4/+
+/cHS4
counts
B220
37%
37%
34%
38%
36%
B220
CD43
PreB
ProB
69%
31%
67%
33%
67%
33%
72%
28%
70%
30%
B220+ IgM-
B cells
ProB cells
PreB cells
% of B220+ cells
% of B220+ IgM- CD43High cells
% of B220+ IgM- CD43low cells
ns
B
Spleen
51%
47%
50%
47%
53%
IgM
49%
43%
48%
45%
51%
IgM+
B cells
IgM+ B cells
% of IgM+ cells
C
Bone Marrow
WT a/b
B1-8/+
IgMa
IgMb
18%
18%
0.4%
36%
0.7%
35%
6%
29%
6%
28%
30%
0.5%
B220+
Spleen
49%
46%
0.4%
99%
1%
98%
12%
84%
12%
83%
98%
0.2%

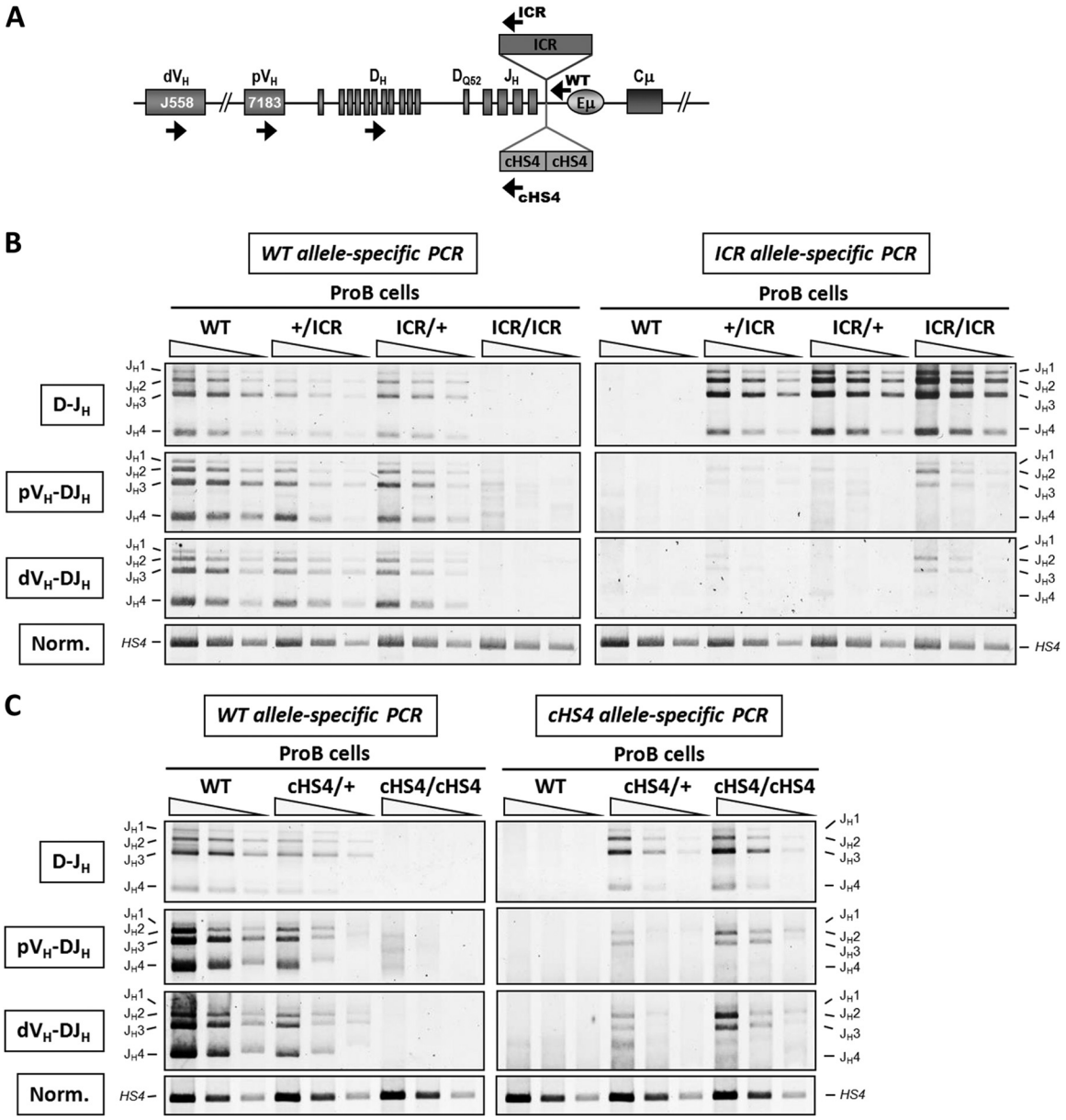

FIG 4 The ICR and cHS4 insertions into the *IgH* locus specifically impair V_H-to-DJ_H recombination. (A) A scheme of the *IgH* locus indicating the relative position of the primers used in PCR. (B) Genomic DNAs were prepared from sorted ICR pro-B cells with the indicated genotypes and were subjected to a semiquantitative PCR to amplify D-J_H and V_H-DJ_H rearrangements. The PCR was performed on serial 3-fold dilutions. A PCR of the HS4 enhancer from the 3′ regulatory region was used for normalization of the DNA input ($n = 3$). (C) Genomic DNAs were prepared from sorted cHS4 pro-B cells and assayed as described in the legend to panel B ($n = 3$).

imal and distal V_H genes on the mutant *ICR* and *cHS4* alleles (Fig. 4B and C).

Our allelic analysis of V(D)J recombination established that the ICR and cHS4 insertions had no significant effect on D-J_H recombination but severely reduced V_H-DJ_H recombination of both the proximal and the distal V_H genes.

Increased sense and decreased antisense germ line transcription at distal V_H genes on the mutant alleles. Previous studies

FIG 3 B cell development, allelic exclusion, and competition in hemizygous mice. (A) Single-cell suspensions from bone marrow with the indicated genotypes were stained with anti-B220 (top) or with anti-$B220^+$, anti-$CD43^+$, and anti-IgM (middle) and gated on the $B220^+$ IgM-negative (IgM^-) population. (Bottom) The histograms show the standard errors ($n = 3$). ns, not significant. (B) Single-cell suspensions from spleen with the indicated genotypes were stained with anti-B220 (top) or with anti-$B220^+$ anti-IgM (middle). (Bottom) The histograms show the standard errors ($n = 3$). (C) Allelic exclusion. Single-cell suspensions from bone marrow (top) or spleen (bottom) of mice with the indicated genotypes were stained with anti-B220 and MAbs against the IgM^a and IgM^b allotypes and gated on the $B220^+$ population ($n = 6$; for *cHS4/+* cells, $n = 2$).

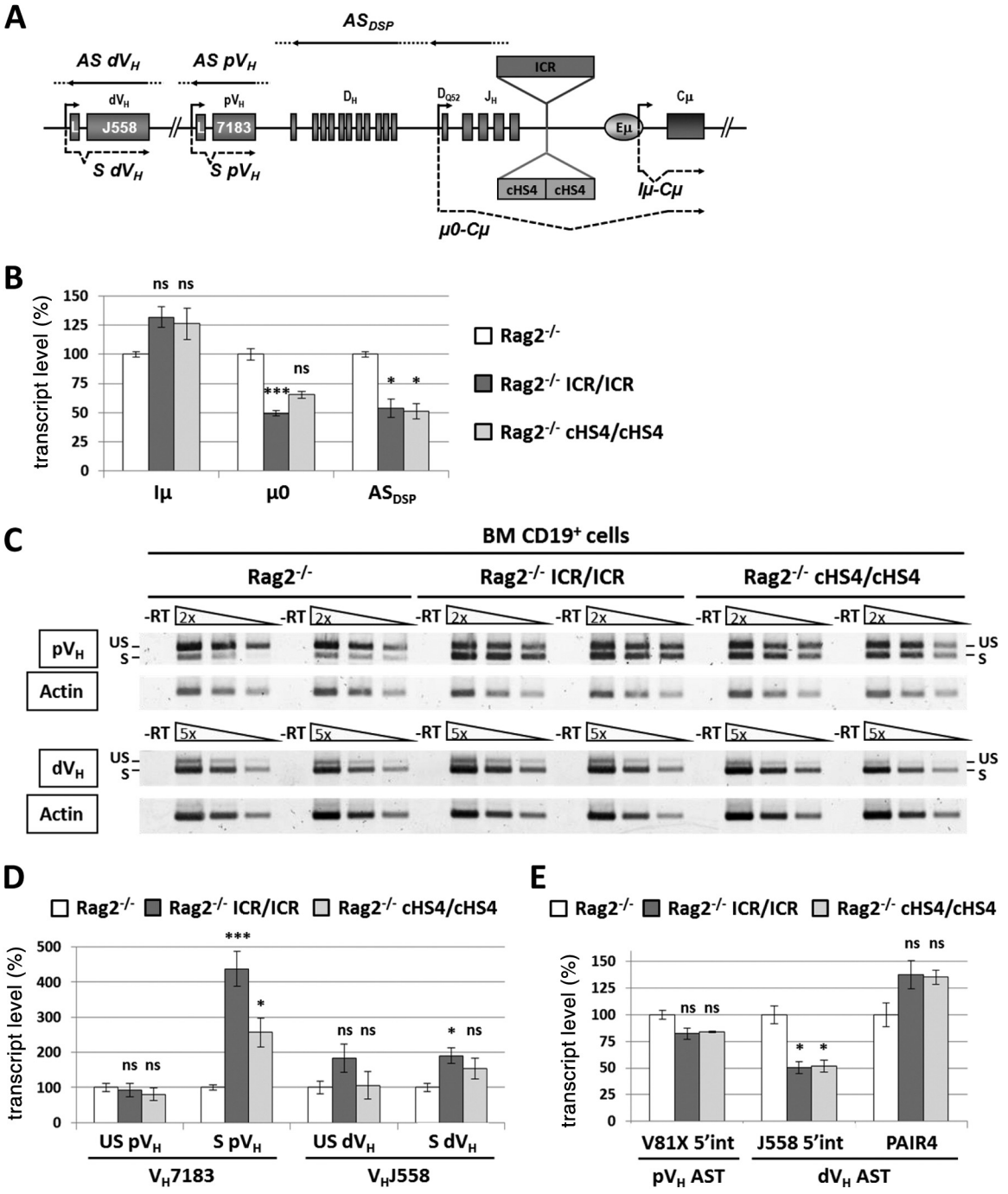

FIG 5 Sense and antisense germ line transcription at V_H genes on the mutant allele. (A) The scheme shows some of the germ line transcripts analyzed at the mutant *IgH* locus. Dots indicate that the initiation and termination sites of the indicated transcripts have not been mapped yet. L, leader; S, sense; AS, antisense. (B) Total RNA from sorted CD19$^+$ cells from the bone marrow of *Rag2*$^{-/-}$, *Rag2*$^{-/-}$ *ICR/ICR*, and *Rag2*$^{-/-}$ *cHS4/cHS4* mice was assayed by RT-qPCR for the indicated transcripts. The corresponding transcript levels in the *Rag2*$^{-/-}$ controls were set at 100% of the signal. *Gapdh* (glyceraldehyde-3-phosphate dehydrogenase gene) and *Ywhaz* (tyrosine 3-monooxygenase/tryptophan 5-monooxygenase activation protein zeta gene) expression was used for normalization. The histograms show the standard errors ($n \geq 4$). ***, $P < 0.001$; *, $P < 0.05$; ns, not significant. (C) Analysis of proximal V_H (pV_H; top) and distal V_H (dV_H; bottom) germ line transcripts by semiquantitative RT-PCR. Two independent samples from each genotype are shown. −RT, no reverse transcription; S, spliced transcripts; US, unspliced (antisense/primary sense) transcripts. (D) Quantification of germ line transcripts of proximal and distal V_H genes by semiquantitative PCR. The signals of the corresponding transcripts in the *Rag2*$^{-/-}$ controls were set at 100%. The histograms show the standard errors ($n \geq 4$). ***, $P < 0.001$; *, $P < 0.05$. (E) Quantification by qPCR of ASTs within the indicated regions of the *IgH* variable locus. The histograms show the standard errors ($n \geq 4$). *, $P < 0.05$. int, intergenic.

showed that deletion of the Eμ enhancer drastically affected μ0 and Iμ STs, derived from the D_{Q52} and Iμ germ line promoters, respectively; ASTs across the D-J_H domain; and a set of proximal V_H germ line transcripts (10–14) (Fig. 5A). To investigate the effect of the ICR and cHS4 insertions on germ line transcription, homozygous ICR and cHS4 mice were brought into a Rag2-deficient background. While Iμ ST levels did not markedly vary regardless of the genotype (Fig. 5B), μ0 ST and DSP AST levels were mildly reduced (~2-fold) in ICR/Rag2 and cHS4/Rag2 mutants (Fig. 5B).

For proximal V_H germ line transcripts, we found an increase in spliced ST levels in ICR/Rag2 and cHS4/Rag2 mice (~4-fold and ~3-fold, respectively) (Fig. 5C and D). In contrast, the levels of unspliced transcripts (covering both ASTs and primary STs) (Fig. 5C and D) and the exclusively antisense V_{H81X} transcripts (the most proximal, functional V_H gene segment) (Fig. 5E) did not vary significantly. For the distal V_H gene transcripts, ST and unspliced transcript levels did not vary markedly under semiquantitative conditions, regardless of the genotype (Fig. 5C and D). By using RT-qPCR to quantify exclusively intergenic ASTs in the distal V_H region, we detected at best a 2-fold decrease within the large J558 family region and no significant variation for the Pax5-activated intergenic repeat 4 (PAIR4) germ line transcripts (28) (Fig. 5E).

Combined, these data establish that insertion of ICR or cHS4 upstream of Eμ has no major effect on the sense and antisense germ line transcripts produced within the D-Cμ domain or within the distal V_H domain but affects the proximal V_H genes, where sense transcripts were upregulated (see Fig. 8).

DJ_H transcription is strongly decreased on the *ICR* and *cHS4* mutant alleles. Taking germ line transcription as a measure of the chromatin accessibility of unrearranged gene segments poised for recombination, the increase of the proximal V_H-specific germ line STs and the relatively normal distal V_H-specific germ line transcripts in ICR and cHS4 mice indicated that it was unlikely that a reduced accessibility of the V_H RSSs was the cause of the impairment of V_H-DJ_H recombination in these mice. This led us to explore the possibility that the ectopic inserts had interfered with DJ_H transcription, potentially rendering the RSSs of the DJ_H segments inaccessible for V_H-DJ_H recombination.

Following D-J_H recombination, the D promoters upstream of assembled DJ_H segments are activated and generate the so-called Dμ transcripts (29, 30). To investigate whether the Dμ transcripts were produced from the excluded allele, we purified B cell populations from ICR × C57BL/6 or cHS4 × C57BL/6 hemizygous mice in which B cell development was driven by the WT IgM^b-expressing allele (the IgM^a-expressing allele in B1-8 × C57BL/6 hemizygous mice) (Fig. 3C).

Since the IgM^b allotype is derived from a productively rearranged WT allele in WT, ICR, and cHS4 hemizygotes (IgM^a from the V_HDJ_{H2} gene in B1-8 hemizygotes), any detectable Dμ transcripts can originate only from the excluded alleles, which can be either in the DJ_H configuration or in a nonproductive V_HDJ_H configuration. Only the former fraction would produce Dμ transcripts, whose spliced forms can be detected by using a degenerate forward primer that pairs with the majority of D-segment RSSs and a Cμ reverse primer (Fig. 6A).

Remarkably, Dμ transcripts were readily detected in WT controls, indicating that expression of the productive allele did not inhibit Dμ transcription on the excluded allele. Dμ transcript levels in B1-8 hemizygotes were slightly superior to those in the WT controls (Fig. 6B), likely reflecting a lower proportion of nonproductive rearrangements on the excluded allele. In stark contrast, the levels of the Dμ transcripts were decreased at least 10 times in ICR and cHS4 hemizygotes (Fig. 6B). The drop of Dμ transcript levels was also evident in ICR and cHS4 homozygous pro-B cells, excluding the possibility of any selection bias as a reason for this drop (Fig. 6C; see Fig. 8). We also quantified mature μ ($V_HDJ_HC\mu$) transcripts (derived from the PV_H promoter following V_H-DJ_H recombination) in sorted pro-B cells and found a severe reduction in ICR cells and a milder decrease in cHS4 pro-B cells for both the proximal and the distal V_H genes (Fig. 6D).

The data reveal a strong inhibition of DJ_H transcription on the excluded *ICR* and *cHS4* mutant alleles.

The ICR affects DNA methylation at DJ_H recombination intermediates in a parent-of-origin manner. The marked decrease of DJ_H transcription on the *ICR* mutant alleles regardless of their parental origin (Fig. 6B and C) led us to investigate the methylation state of DJ_H segments on the excluded alleles. To this end, *ICR/ICR* homozygous mice were crossed with B1-8/B1-8 mice. In the resulting progeny, the *ICR* mutant allele was totally excluded independently of its parental origin (Fig. 3C and D). To analyze the methylation pattern of the excluded alleles, genomic DNAs were extracted from bone marrow B cells of B1-8/+, B1-8/ICR, and ICR/B1-8 mice and assayed by bisulfite sequencing. We first ascertained that the paternal but not the maternal ectopic ICR was heavily methylated (Fig. 7A and B). We also verified that DNA methylation at the ectopic ICR on the excluded, paternal allele had not spread into the Eμ enhancer. Indeed, the Eμ enhancer was unmethylated regardless of the genotype (Fig. 7C). Interestingly, while the unrearranged J_{H1} region was fully methylated (Fig. 7D), the rearranged J_{H1} segment on the excluded allele displayed different methylation patterns depending on the genotype. In B1-8/+ mice, it was demethylated, suggesting that allelic exclusion in this system did not correlate with methylation of the excluded DJ_H allele. In contrast, in both ICR/B1-8 and B1-8/ICR mice, the rearranged J_{H1} segment remained heavily methylated (Fig. 7E and F). Strikingly, the rearranged D segments on the excluded alleles were unmethylated in B1-8/ICR mice but were heavily methylated in ICR/B1-8 mice. This pattern was more obvious for the rearranged $D_{FL16.1}$ segment, which retained its upstream CpG, as it is the 5′-most functional D segment (Fig. 7E and F). The untemplated CpGs, added by the terminal deoxynucleotidyl transferase during V(D)J recombination, were consistently methylated (Fig. 7E and F) (see Discussion).

Thus, in contrast to the excluded wild-type allele, the rearranged J_{H1} segment remains fully methylated on the excluded *ICR* allele. Moreover, when the ectopic ICR binds CTCF, the rearranged DJ_H segment on the excluded allele is methylated. In contrast, when the ectopic ICR is methylated, the aberrant DNA methylation is highly confined to the rearranged J_{H1} segment.

DISCUSSION

Our main finding is that ectopic insertion of either the imprinted *H19* ICR or the cHS4 insulator upstream of the Eμ enhancer leads to a severe impairment of V_H-DJ_H recombination and an almost complete ablation of DJ_H transcription. For the first time, our experimental *in vivo* system reveals a strong correlation between reduced DJ_H transcription and impairment of V_H-DJ_H recombination. We do not infer that this is the sole mechanism explaining

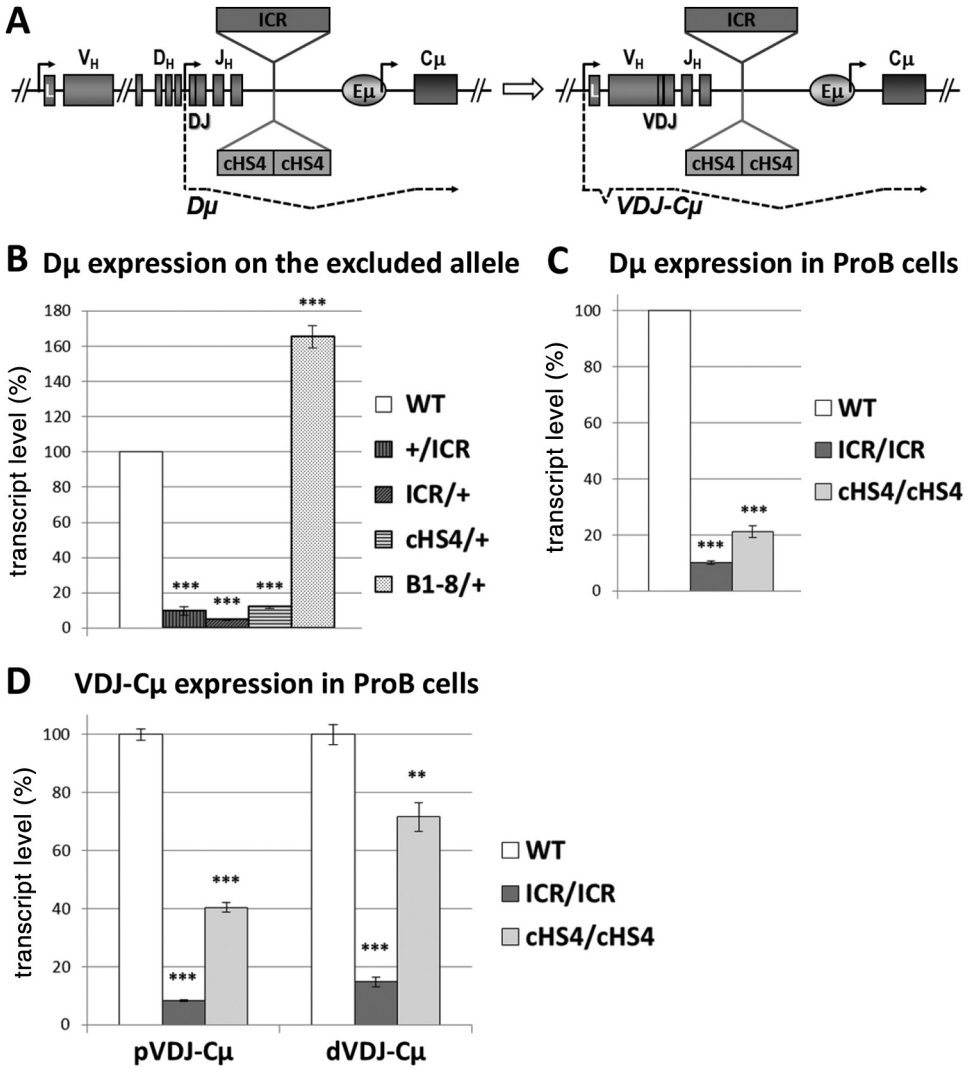

FIG 6 DJ_H transcription is strongly decreased on the excluded alleles. (A) A scheme showing a partially (DJ_{H2}) rearranged *IgH* locus and the resulting DJ_H transcript (Dμ) and a fully (V_HDJ_{H2}) rearranged gene and the resulting VDJ-Cμ transcript. (B) $B220^+$, AA4.1-positive ($AA4.1^+$), and IgM^b-positive (IgM^{b+}) B cells from the bone marrow of hemizygous mice with the indicated genotypes were sorted ($B220^+$, $AA4.1^+$, and IgM^a-positive [IgM^{a+}] B cells were used for B1-8/+ mice). The WT allele is derived from C57BL/6 mice. Total RNA was extracted and reverse transcribed. Spliced DJ_H transcripts were quantified by qPCR. WT transcript levels were set as 100% of the signal. *Gapdh* and *Ywhaz* transcripts were used for normalization. The histograms show the standard errors ($n = 3$). ***, $P < 0.001$. (C) RNA from sorted homozygous pro-B cells was assayed as described in the legend to panel B ($n = 3$). ***, $P < 0.001$. (D) RNA from sorted homozygous pro-B cells was assayed as described in the legend to panel B ($n = 3$). ***, $P < 0.001$; **, $P < 0.01$.

the reduced V_H-DJ_H recombination in our mutants, as other mechanisms underlying, for instance, the architecture of the *IgH* locus (31, 32) could also be involved.

Another key finding of this study is that the *H19* ICR faithfully recapitulates the main epigenetic features of its endogenous counterpart. On the maternal allele, the ectopic ICR binds CTCF/cohesins. During spermatogenesis, just like the endogenous ICR, the ectopic ICR acquires DNA methylation. This paternal methylation is stably maintained in the embryo and during development into B cells. In the context of the *IgH* locus, therefore, the ~2.4-kb ICR fragment seems to have all the requirements for the recruitment of the *de novo* methyltransferase Dnmt3a and its cofactor, Dnmt3L, which mediate establishment of imprinted DNA methylation at ICRs (20, 33). Our findings differ from previous reports, where insertions of the *H19* ICR into other ectopic loci or in transgenic systems were found to acquire DNA methylation after fertilization only (34–37). How the ectopic ICR recruits the DNA methyltransferase complex in developing male germ cells remains unclear. At the endogenous locus, this process is associated with transcription through the ICR (19), but there is no evidence that the *IgH* locus is transcriptionally active in fetal male germ cells. It seems unlikely that the insertion site at the *IgH* locus dictates DNA methylation because the cHS4 insulator remained completely unmethylated at the same site. Rather, our observations suggest that DNA methylation acquisition at the ectopic ICR is an active process that is specifically targeted by the ICR sequence itself.

The inserted ICR exerted its phenotypic effects regardless of its parental origin. This unexpected finding was not related to DNA insertion *per se*, since insertion of cHS4, which has a similar size, did not yield the same phenotype. Moreover, insertion of the *Neo*^{r}

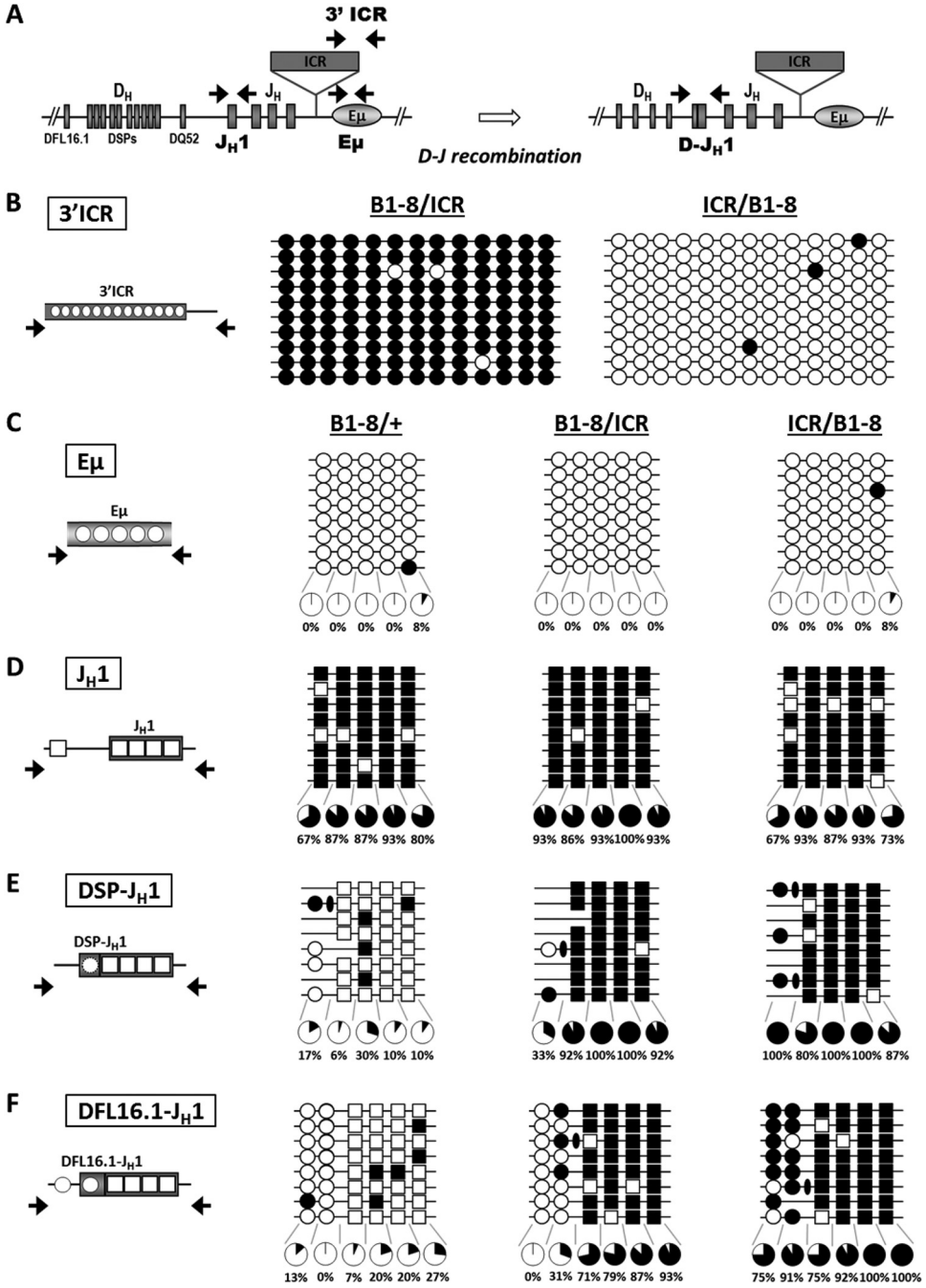

FIG 7 DNA methylation patterns of DJ_H segments are differentially affected by the paternal and maternal ectopic ICR. Genomic DNAs from bone marrow B cells of B1-8/+, B1-8/ICR, and ICR/B1-8 mice were assayed by bisulfite sequencing. (A) The scheme shows the localization of the primer pairs used prior to and after D-J_H recombination. (B to F) The analyzed CpGs are displayed in the left panel. Methylated CpGs are indicated by filled circles or squares. Unmethylated CpGs are indicated by open circles or squares. The percentages are based on 15 individual sequences for each region derived from two independent pools of mice. Representative sets of sequences are shown. (B) Methylation status of 13 CpGs at the 3′ part of the ectopic *H19* ICR is shown. (C) Results of bisulfite sequencing of the Eμ region from mice of the indicated genotypes. (D) Methylation of CpGs of the unrearranged J_{H1} region. Note that 4 CpGs lie within and 1 CpG lies right upstream of the J_{H1} segment. The latter is deleted upon any D-J_{H1} recombination event. (E and F) DNA methylation of DJ_H recombination intermediates involving DSP segments (E) or the DFL16.1 segment (F). Circles, CpGs of the D segments; squares, CpGs of the J_{H1} segment; ovals, the nontemplated CpGs added during D-J_{H1} recombination. Note that the 5′-most CpG of the DFL16.1 segment lies within the promoter region and is not lost upon DFL16.1-J_{H1} recombination. Throughout, the clonality of the sequences was established on the basis of sequence diversity at D-J_{H1} junctions. Sequences with identical junctions were counted as one.

gene at different sites upstream of Eμ led to qualitatively different effects on germ line transcription and V(D)J recombination (38, 39).

Whereas potential CTCF-mediated looping from the maternal ICR to other CTCF-binding sites at the *IgH* locus may be envisaged on the maternal chromosome, the long- and short-range effects of the methylated, paternal ICR were unexpected. These effects were clearly not due to an altered Eμ configuration, since

this enhancer was still transcribed and unmethylated. One plausible explanation for the phenotypic effect of the paternal inheritance of the inserted ICR comes from a recent targeting study in the mouse (40), which shows that the methylated paternal allele of the *H19* ICR exerts a repressive effect in *cis* on transcription. It remains to be discovered what precisely mediates the repressive *cis* effects of the methylated *H19* ICR after D-J_H recombination and whether this could be related to the density of CpGs and/or the binding of methyl CpG binding domain (MBD) proteins.

Not only in the *ICR*/+ hemizygotes but also in the +/*ICR* hemizygotes, DJ_H transcription was severely reduced on the mutated allele. Significantly, a recent comprehensive analysis of DNA methylation revealed widespread CpG methylation at the D-Eμ domain prior to V(D)J recombination, but the Eμ and the D_{Q52} promoter remained unmethylated at this developmental stage (25). After D-J_H recombination, however, Eμ-mediated demethylation occurred specifically at the recombined DJ_H segments (25). We find that this demethylation process was affected in both +/*ICR* and *ICR*/+ hemizygous mice.

Particularly, on the excluded paternal *ICR* allele, there was highly confined DNA methylation at the rearranged J_{H1} segment. The single CpG dinucleotide in the promoter region of the $D_{FL16.1}$ segment was consistently unmethylated. This suggests that the promoter is, at least with regard to DNA methylation, in an open configuration. On the excluded maternal *ICR* allele, in *ICR*/+ mice, DNA methylation spanning both rearranged D and J_{H1} segments occurred, a situation that is reminiscent of the reported Eμ deletion effect (25). Regardless of the parental origin of the ectopic ICR, however, the aberrant DNA methylation was clearly polarized toward upstream sequences. The Eμ enhancer itself remained fully unmethylated on the excluded alleles. Together, these data indicate that the ectopic ICR differentially affects the demethylation of recombined DJ_H segments and, as a corollary, that the demethylating activity of the Eμ enhancer was differentially impaired by the ectopic ICR insertion.

The observed aberrant methylation states of DJ_H recombination intermediates correlated with a dramatic reduction of DJ_H transcription. Despite this clear correlation, we think that reduced DJ_H transcription, rather than the aberrant DJ_H methylation, accounts best for the observed reduced V_H-DJ_H recombination. The RAG complex is able to efficiently catalyze D-J_H recombination, despite extensive methylation of germ line D segments (with the exception of D_{Q52}) and J_H segments (25; this study). Therefore, it is difficult to envisage that methylation of DJ_H segments *per se* would hamper the action of RAG complexes. Additionally, the lack of a correlation between DNA methylation, on the one hand, and germ line transcription, active histone marks, and the recombination potential of germ line D and J_H segments (25, 41), on the other hand, leads us to suggest that Eμ controls DJ_H transcription and demethylation by distinct mechanisms. This should be relevant for further exploration in future studies.

We found in our study that in a Rag2-deficient background, there was only a mild decrease of germ line transcription within the D-Cμ domain and, in Rag2-proficient pro-B cells, D-J_H recombination was unaffected. These findings indicate that neither the ICR nor the cHS4 insertion interfered in a major way with the accessibility control function of Eμ within the D-Cμ domain or with the recruitment of the RAG complex for the first, D-J_H, recombination step. Indeed, this process was unaffected.

Previous studies have shown that deletion of the Eμ enhancer impaired D-J_H recombination and more severely V_H-DJ_H recombination (10, 11). These findings led to the proposal that impaired V_H-DJ_H recombination was a downstream consequence of the primary block in D-J_H recombination (10). We found that it was transcription of DJ_H segments and not D-J_H recombination itself which was severely reduced in the ICR and cHS4 mice. This key finding highlights the importance of DJ_H transcription in V_H-DJ_H recombination.

Our combined data favor the view that Eμ is developmentally bimodal in its action (Fig. 8). Prior to D-J_H recombination, Eμ controls germ line transcription within the D-Cμ domain and of a set of proximal V_H genes as far away as 400 kb (13), despite the presence of the insulators (our study) and CTCF/cohesin binding at IGCR1 CBEs (16–18). Moreover, while deletion of Eμ induced a drastic reduction of μ0 ST and DSP ASTs (11, 12), we found only a mild reduction of these transcripts. After D-J_H recombination, however, Eμ activity was focused on the nearby DJ_H promoter and was particularly sensitive to the insulators' blocker effect (Fig. 8). It should be noted that D-J_H recombination brings the DJ_H promoter close to the inserted insulators (at ~1.8 kb for DJ_{H4} and ~3.2 kb for DJ_{H1}), whereas the D_{Q52} promoter is ~3.6 kb from the ICR and cHS4. The fact that μ0 transcripts were only modestly affected, whereas Dμ transcripts were severely reduced, further suggests that the Eμ enhancer is developmentally programmed to shift its activity after DJ_H rearrangement. Additionally, any D-J_H recombination not involving D_{Q52} brings closer the heterochromatic marks associated with the far upstream DSP segments (42), which may spread to the DJ_H promoter. In the absence of counteracting active chromatin marks normally promoted by Eμ (13), the DJ_H promoter may become silenced.

Our Eμ bimodal activity model predicts that after V_H-DJ_H recombination, Eμ-mediated effects shift to the PV_H promoter of the rearranged V(D)J exon. In support of this prediction, μ gene transcript levels were reported to be reduced in the bone marrow in the absence of Eμ or when this element is insulated (43; this study).

The correlation between V_H sense and antisense germ line transcription and V_H recombination is still unclear (10–15, 18, 44–49). Deletion of the whole V_H-D intergenic region led to an increase of proximal V_H-DJ_H recombination which correlated with increased antisense germ line transcription originating from the D cluster and spanning the now close by proximal V_H genes (15). In contrast, the increased proximal V_H-DJ_H recombination in mice devoid of the IGCR1 CTCF sites was associated with increased sense germ line transcription of proximal V_H genes (18). Interestingly, in both ICR and cHS4 mice, an increased sense germ line transcription of proximal V_H genes was seen. This hints to the possibility that the ectopic sequences are engaged in a CTCF-mediated interaction with the IGCR1. However, this hypothesis cannot explain the similar effect conveyed by the paternal ectopic ICR, which rather points to a distinct, CTCF-independent mechanism. Notwithstanding, in our study, the reduction of proximal V_H-DJ_H recombination was seen, despite increased sense and normal antisense germ line transcription. This suggests that the accessibility of proximal V_H genes, at least as measured by transcription, was not the limiting factor in the ICR and cHS4 mice, and this emphasizes again the likely importance of the defect in DJ_H transcription.

Within the distal V_H domain, overall normal ST and AST levels did not correlate with an efficient distal V_H-DJ_H recombination,

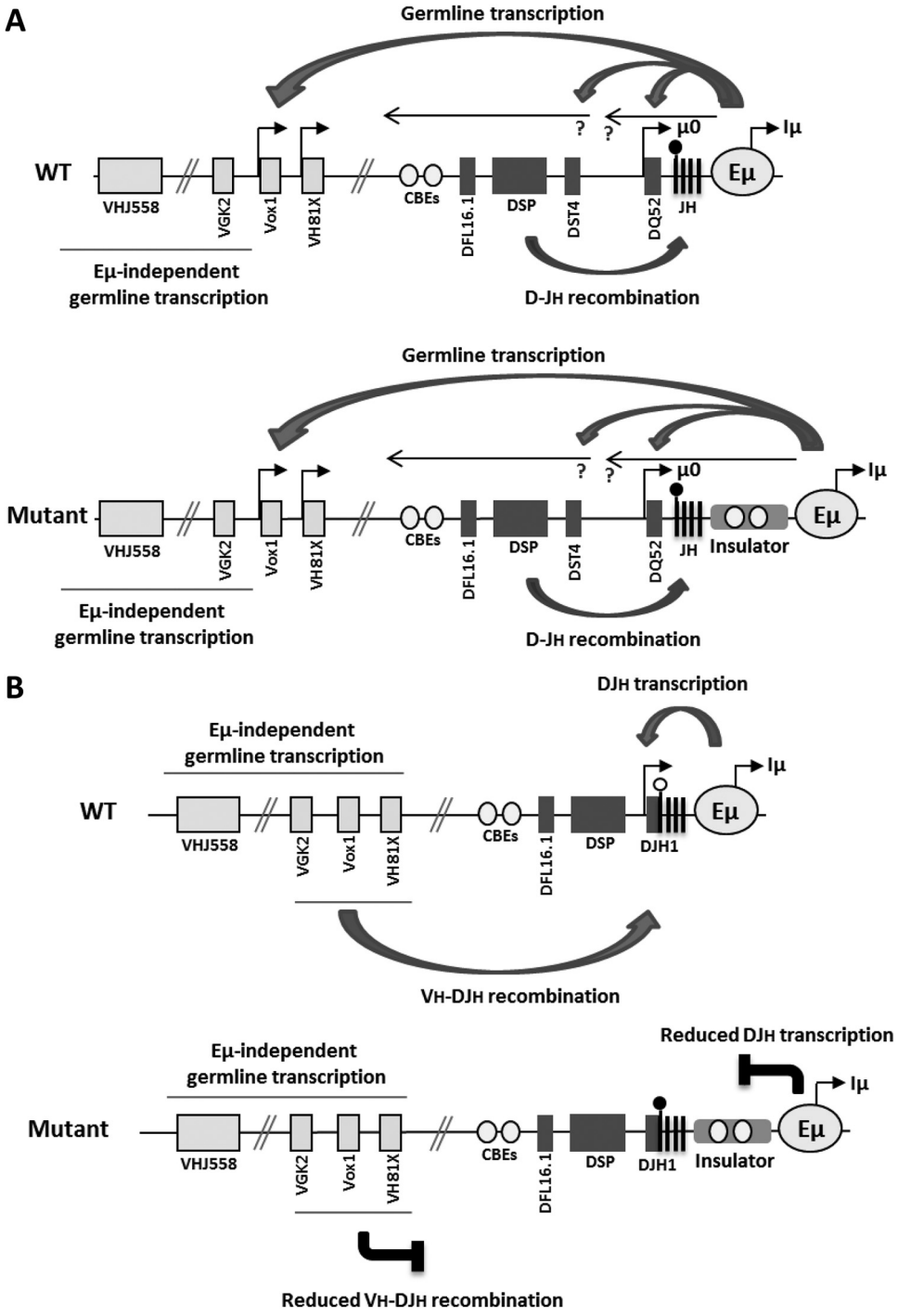

FIG 8 An Eμ bimodal activity model. This working model stipulates that Eμ activity shifts during early B cell development. (A) Prior to D-J_H recombination, the Eμ enhancer controls sense and antisense transcription within the D-Cμ chromatin domain and sense transcription of a set of proximal V_H gene segments that are more than 400 kb away. Eμ also controls D-J_H recombination. Neither of the activities of the Eμ enhancer is hampered by either the IGCR1 CTCF/cohesin sites or the ectopic insulators. (B) After D-J_H recombination, Eμ activity is focused on the nearby DJ_H promoter and becomes sensitive to the insulators' blocker effect. The control of DJ_H transcription is crucial for V_H-DJ_H recombination and allelic exclusion. The arrows indicate only the sense and antisense transcripts which were shown to be controlled by the Eμ enhancer. The question marks mean that initiation and termination of the indicated antisense transcripts have not been unambiguously defined. The CpG of the J_{H1} segment is shown as a filled (methylated) or empty (unmethylated) lollipop. CBEs denote CTCF-binding elements within the intergenic control region (IGCR1) upstream of DFL16.1. The figure was compiled from information presented in references 12 to 18 and the present study.

despite the accessibility of the V_H RSSs. Again, this clearly shows that V_H transcription *per se* is not sufficient for V(D)J recombination. This is in agreement with the results of previous studies, which did not find a causal relationship between germ line transcription of distal V_H genes and their recombination. Indeed, distal V_H-DJ_H recombination was reduced in different mutants (including mutants with the deletion of Eμ, IGCR1 CTCF sites, Pax5, EZH2, Ikaros, and YY1) that displayed apparently unchanged

(11–13, 18, 45, 46), seemingly increased (48), or reduced (47, 49) distal V_H transcription.

In the context of allelic competition, the reduced efficiency with which the *ICR* and, to a lesser extent, the *cHS4* mutant alleles undergo V_H-DJ_H recombination may be explained by reduced DJ_H transcription. This may indicate that the latter is a mark of the excluded allele. However, the high levels of DJ_H transcripts from the excluded alleles in WT and B1-8 hemizygotes showed the opposite. Thus, the complete exclusion of the *ICR* mutant allele may actually result from two additive yet distinct mechanisms: a transcriptional silencing upon D-J_H recombination, leading to a defective allele, followed by enforcement by allelic exclusion. In support of this notion, the *cHS4* allele could sustain some allelic competition, and the levels of DJ_H transcripts on the excluded *cHS4* allele were relatively higher than those on the *ICR* allele.

Our findings strongly suggest that genuine allelic exclusion requires efficient DJ_H transcription. Functionally, this would ensure that the DJ_H RSSs of the second allele will be available if V_H-DJ_H recombination on the first allele is not productive. We propose that one mechanism by which the Eμ enhancer controls allelic exclusion could be through the control of DJ_H transcription levels, which should be interesting to explore further in future studies.

ACKNOWLEDGMENTS

We thank F. W. Alt for providing genomic DNA from IGCR1-deficient mice and K. Rajewsky for the B1-8 mouse line. We also thank P. Mercier and M. Philippe at the IPBS transgenesis platform and F. L'Faqihi and V. Duplan-Eche at the Purpan CPTP platform for their excellent work and J. Tessier for his help with embryonic stem cell transfections. We thank M. Moutahir for handling the mouse lines.

This work was supported by grants from the INCa, ANR, the Fondation ARC, the Ligue Contre le Cancer-Comité de Haute-Garonne, and the Cancéropôle GSO. N.-S.N.H. was supported by a fellowship from INCa, and R.H. was supported by a fellowship from the Japan Society for the Promotion of Science Postdoctoral Fellowships for Research Abroad. R.F. is associated with the Labex EpiGenMed and the European NoE EpiGeneSys.

We declare that we have no conflict of interest.

REFERENCES

1. **Goldmit M, Bergman Y.** 2004. Monoallelic gene expression: a repertoire of recurrent themes. Immunol Rev **200:**197–214. http://dx.doi.org/10.1111/j.0105-2896.2004.00158.x.
2. **Yang PK, Kuroda MI.** 2007. Noncoding RNAs and intranuclear positioning in monoallelic gene expression. Cell **128:**777–786. http://dx.doi.org/10.1016/j.cell.2007.01.032.
3. **Delaval K, Feil R.** 2004. Epigenetic regulation of mammalian genomic imprinting. Curr Opin Genet Dev **14:**188–195. http://dx.doi.org/10.1016/j.gde.2004.01.005.
4. **Jung D, Giallourakis C, Mostoslavsky R, Alt FW.** 2006. Mechanism and control of V(D)J recombination at the immunoglobulin heavy chain locus. Annu Rev Immunol **24:**541–570. http://dx.doi.org/10.1146/annurev.immunol.23.021704.115830.
5. **Schatz DG, Ji Y.** 2011. Recombination centres and the orchestration of V(D)J recombination. Nat Rev Immunol **11:**251–263. http://dx.doi.org/10.1038/nri2941.
6. **Vettermann C, Schlissel MS.** 2010. Allelic exclusion of immunoglobulin genes: models and mechanisms. Immunol Rev **237:**22–42. http://dx.doi.org/10.1111/j.1600-065X.2010.00935.x.
7. **Johnston CM, Wood AL, Bolland DJ, Corcoran AE.** 2006. Complete sequence assembly and characterization of the C57BL/6 mouse Ig heavy chain V region. J Immunol **176:**4221–4234. http://dx.doi.org/10.4049/jimmunol.176.7.4221.
8. **Retter I, Chevillard C, Scharfe M, Conrad A, Hafner M, Im TH, Ludewig M, Nordsiek G, Severitt S, Thies S, Mauhar A, Blocker H, Muller W, Riblet R.** 2007. Sequence and characterization of the Ig heavy chain constant and partial variable region of the mouse strain 129S1. J Immunol **179:**2419–2427. http://dx.doi.org/10.4049/jimmunol.179.4.2419.
9. **Cobb RM, Oestreich KJ, Osipovich OA, Oltz EM.** 2006. Accessibility control of V(D)J recombination. Adv Immunol **91:**45–109. http://dx.doi.org/10.1016/S0065-2776(06)91002-5.
10. **Afshar R, Pierce S, Bolland DJ, Corcoran A, Oltz EM.** 2006. Regulation of IgH gene assembly: role of the intronic enhancer and 5′DQ52 region in targeting DHJH recombination. J Immunol **176:**2439–2447. http://dx.doi.org/10.4049/jimmunol.176.4.2439.
11. **Perlot T, Alt FW, Bassing CH, Suh H, Pinaud E.** 2005. Elucidation of IgH intronic enhancer functions via germ-line deletion. Proc Natl Acad Sci U S A **102:**14362–14367. http://dx.doi.org/10.1073/pnas.0507090102.
12. **Bolland DJ, Wood AL, Afshar R, Featherstone K, Oltz EM, Corcoran AE.** 2007. Antisense intergenic transcription precedes IgH D-to-J recombination and is controlled by the intronic enhancer Emu. Mol Cell Biol **27:**5523–5533. http://dx.doi.org/10.1128/MCB.02407-06.
13. **Chakraborty T, Perlot T, Subrahmanyam R, Jani A, Goff PH, Zhang Y, Ivanova I, Alt FW, Sen R.** 2009. A 220-nucleotide deletion of the intronic enhancer reveals an epigenetic hierarchy in immunoglobulin heavy chain locus activation. J Exp Med **206:**1019–1027. http://dx.doi.org/10.1084/jem.20081621.
14. **Perlot T, Li G, Alt FW.** 2008. Antisense transcripts from immunoglobulin heavy-chain locus V(D)J and switch regions. Proc Natl Acad Sci U S A **105:**3843–3848. http://dx.doi.org/10.1073/pnas.0712291105.
15. **Giallourakis CC, Franklin A, Guo C, Cheng HL, Yoon HS, Gallagher M, Perlot T, Andzelm M, Murphy AJ, Macdonald LE, Yancopoulos GD, Alt FW.** 2010. Elements between the IgH variable (V) and diversity (D) clusters influence antisense transcription and lineage-specific V(D)J recombination. Proc Natl Acad Sci U S A **107:**22207–22212. http://dx.doi.org/10.1073/pnas.1015954107.
16. **Degner SC, Wong TP, Jankevicius G, Feeney AJ.** 2009. Cutting edge: developmental stage-specific recruitment of cohesin to CTCF sites throughout immunoglobulin loci during B lymphocyte development. J Immunol **182:**44–48. http://dx.doi.org/10.4049/jimmunol.182.1.44.
17. **Featherstone K, Wood AL, Bowen AJ, Corcoran AE.** 2010. The mouse immunoglobulin heavy chain V-D intergenic sequence contains insulators that may regulate ordered V(D)J recombination. J Biol Chem **285:**9327–9338. http://dx.doi.org/10.1074/jbc.M109.098251.
18. **Guo C, Yoon HS, Franklin A, Jain S, Ebert A, Cheng HL, Hansen E, Despo O, Bossen C, Vettermann C, Bates JG, Richards N, Myers D, Patel H, Gallagher M, Schlissel MS, Murre C, Busslinger M, Giallourakis CC, Alt FW.** 2011. CTCF-binding elements mediate control of V(D)J recombination. Nature **477:**424–430. http://dx.doi.org/10.1038/nature10495.
19. **Henckel A, Chebli K, Kota SK, Arnaud P, Feil R.** 2012. Transcription and histone methylation changes correlate with imprint acquisition in male germ cells. EMBO J **31:**606–615. http://dx.doi.org/10.1038/emboj.2011.425.
20. **Kota SK, Feil R.** 2010. Epigenetic transitions in germ cell development and meiosis. Dev Cell **19:**675–686. http://dx.doi.org/10.1016/j.devcel.2010.10.009.
21. **Bell AC, West AG, Felsenfeld G.** 1999. The protein CTCF is required for the enhancer blocking activity of vertebrate insulators. Cell **98:**387–396. http://dx.doi.org/10.1016/S0092-8674(00)81967-4.
22. **Szabo PE, Tang SH, Reed MR, Silva FJ, Tsark WM, Mann JR.** 2002. The chicken beta-globin insulator element conveys chromatin boundary activity but not imprinting at the mouse Igf2/H19 domain. Development **129:**897–904.
23. **Dickson J, Gowher H, Strogantsev R, Gaszner M, Hair A, Felsenfeld G, West AG.** 2010. VEZF1 elements mediate protection from DNA methylation. PLoS Genet **6:**e1000804. http://dx.doi.org/10.1371/journal.pgen.1000804.
24. **Kirillov A, Kistler B, Mostoslavsky R, Cedar H, Wirth T, Bergman Y.** 1996. A role for nuclear NF-kappaB in B-cell-specific demethylation of the Igkappa locus. Nat Genet **13:**435–441. http://dx.doi.org/10.1038/ng0895-435.
25. **Selimyan R, Gerstein RM, Ivanova I, Precht P, Subrahmanyam R, Perlot T, Alt FW, Sen R.** 2013. Localized DNA demethylation at recombination intermediates during immunoglobulin heavy chain gene assembly. PLoS Biol **11:**e1001475. http://dx.doi.org/10.1371/journal.pbio.1001475.
26. **von Boehmer H, Melchers F.** 2010. Checkpoints in lymphocyte develop-

ment and autoimmune disease. Nat Immunol **11:**14–20. http://dx.doi.org/10.1038/ni.1794.
27. **Sonoda E, Pewzner-Jung Y, Schwers S, Taki S, Jung S, Eilat D, Rajewsky K.** 1997. B cell development under the condition of allelic inclusion. Immunity **6:**225–233. http://dx.doi.org/10.1016/S1074-7613(00)80325-8.
28. **Ebert A, McManus S, Tagoh H, Medvedovic J, Salvagiotto G, Novatchkova M, Tamir I, Sommer A, Jaritz M, Busslinger M.** 2011. The distal V(H) gene cluster of the IgH locus contains distinct regulatory elements with Pax5 transcription factor-dependent activity in pro-B cells. Immunity **34:**175–187. http://dx.doi.org/10.1016/j.immuni.2011.02.005.
29. **Reth MG, Alt FW.** 1984. Novel immunoglobulin heavy chains are produced from DJH gene segment rearrangements in lymphoid cells. Nature **312:**418–423. http://dx.doi.org/10.1038/312418a0.
30. **Alessandrini A, Desiderio SV.** 1991. Coordination of immunoglobulin DJH transcription and D-to-JH rearrangement by promoter-enhancer approximation. Mol Cell Biol **11:**2096–2107.
31. **Guo C, Gerasimova T, Hao H, Ivanova I, Chakraborty T, Selimyan R, Oltz EM, Sen R.** 2011. Two forms of loops generate the chromatin conformation of the immunoglobulin heavy-chain gene locus. Cell **147:**332–343. http://dx.doi.org/10.1016/j.cell.2011.08.049.
32. **Medvedovic J, Ebert A, Tagoh H, Tamir IM, Schwickert TA, Novatchkova M, Sun Q, Huis In't Veld PJ, Guo C, Yoon HS, Denizot Y, Holwerda SJ, de Laat W, Cogne M, Shi Y, Alt FW, Busslinger M.** 2013. Flexible long-range loops in the VH gene region of the IgH locus facilitate the generation of a diverse antibody repertoire. Immunity **39:**229–244. http://dx.doi.org/10.1016/j.immuni.2013.08.011.
33. **Sasaki H, Matsui Y.** 2008. Epigenetic events in mammalian germ-cell development: reprogramming and beyond. Nat Rev Genet **9:**129–140. http://dx.doi.org/10.1038/nrg2295.
34. **Gebert C, Kunkel D, Grinberg A, Pfeifer K.** 2010. H19 imprinting control region methylation requires an imprinted environment only in the male germ line. Mol Cell Biol **30:**1108–1115. http://dx.doi.org/10.1128/MCB.00575-09.
35. **Matsuzaki H, Okamura E, Shimotsuma M, Fukamizu A, Tanimoto K.** 2009. A randomly integrated transgenic H19 imprinting control region acquires methylation imprinting independently of its establishment in germ cells. Mol Cell Biol **29:**4595–4603. http://dx.doi.org/10.1128/MCB.00275-09.
36. **Park KY, Sellars EA, Grinberg A, Huang SP, Pfeifer K.** 2004. The H19 differentially methylated region marks the parental origin of a heterologous locus without gametic DNA methylation. Mol Cell Biol **24:**3588–3595. http://dx.doi.org/10.1128/MCB.24.9.3588-3595.2004.
37. **Tanimoto K, Shimotsuma M, Matsuzaki H, Omori A, Bungert J, Engel JD, Fukamizu A.** 2005. Genomic imprinting recapitulated in the human beta-globin locus. Proc Natl Acad Sci U S A **102:**10250–10255. http://dx.doi.org/10.1073/pnas.0409541102.
38. **Chen J, Young F, Bottaro A, Stewart V, Smith RK, Alt FW.** 1993. Mutations of the intronic IgH enhancer and its flanking sequences differentially affect accessibility of the JH locus. EMBO J **12:**4635–4645.
39. **Delpy L, Decourt C, Le Bert M, Cogne M.** 2002. B cell development arrest upon insertion of a neo gene between JH and Emu: promoter competition results in transcriptional silencing of germline JH and complete VDJ rearrangements. J Immunol **169:**6875–6882. http://dx.doi.org/10.4049/jimmunol.169.12.6875.
40. **Ideraabdullah FY, Abramowitz LK, Thorvaldsen JL, Krapp C, Wen SC, Engel N, Bartolomei MS.** 2011. Novel cis-regulatory function in ICR-mediated imprinted repression of H19. Dev Biol **355:**349–357. http://dx.doi.org/10.1016/j.ydbio.2011.04.036.
41. **Subrahmanyam R, Du H, Ivanova I, Chakraborty T, Ji Y, Zhang Y, Alt FW, Schatz DG, Sen R.** 2012. Localized epigenetic changes induced by DH recombination restricts recombinase to DJH junctions. Nat Immunol **13:**1205–1212. http://dx.doi.org/10.1038/ni.2447.
42. **Chakraborty T, Chowdhury D, Keyes A, Jani A, Subrahmanyam R, Ivanova I, Sen R.** 2007. Repeat organization and epigenetic regulation of the DH-Cmu domain of the immunoglobulin heavy-chain gene locus. Mol Cell **27:**842–850. http://dx.doi.org/10.1016/j.molcel.2007.07.010.
43. **Li F, Eckhardt LA.** 2009. A role for the IgH intronic enhancer E mu in enforcing allelic exclusion. J Exp Med **206:**153–167. http://dx.doi.org/10.1084/jem.20081202.
44. **Fuxa M, Skok J, Souabni A, Salvagiotto G, Roldan E, Busslinger M.** 2004. Pax5 induces V-to-DJ rearrangements and locus contraction of the immunoglobulin heavy-chain gene. Genes Dev **18:**411–422. http://dx.doi.org/10.1101/gad.291504.
45. **Hesslein DG, Pflugh DL, Chowdhury D, Bothwell AL, Sen R, Schatz DG.** 2003. Pax5 is required for recombination of transcribed, acetylated, 5′ IgH V gene segments. Genes Dev **17:**37–42. http://dx.doi.org/10.1101/gad.1031403.
46. **Liu H, Schmidt-Supprian M, Shi Y, Hobeika E, Barteneva N, Jumaa H, Pelanda R, Reth M, Skok J, Rajewsky K.** 2007. Yin Yang 1 is a critical regulator of B-cell development. Genes Dev **21:**1179–1189. http://dx.doi.org/10.1101/gad.1529307.
47. **Reynaud D, Demarco IA, Reddy KL, Schjerven H, Bertolino E, Chen Z, Smale ST, Winandy S, Singh H.** 2008. Regulation of B cell fate commitment and immunoglobulin heavy-chain gene rearrangements by Ikaros. Nat Immunol **9:**927–936. http://dx.doi.org/10.1038/ni.1626.
48. **Su IH, Basavaraj A, Krutchinsky AN, Hobert O, Ullrich A, Chait BT, Tarakhovsky A.** 2003. Ezh2 controls B cell development through histone H3 methylation and IgH rearrangement. Nat Immunol **4:**124–131. http://dx.doi.org/10.1038/ni876.
49. **Verma-Gaur J, Torkamani A, Schaffer L, Head SR, Schork NJ, Feeney AJ.** 2012. Noncoding transcription within the IgH distal V(H) region at PAIR elements affects the 3D structure of the IgH locus in pro-B cells. Proc Natl Acad Sci U S A **109:**17004–17009. http://dx.doi.org/10.1073/pnas.1208398109.